

hydroxyadamantan-2-one with isopropylidetriphenylphosphorane (cf. Table I).

To obtain more direct evidence for the one-electron transfer mechanism we also undertook investigation of a possible chemically induced dynamic nuclear polarization (CIDNP) effect in the Wittig reaction. In our attempts we reacted  $\text{Ph}_3\text{P}^+-\text{CH}_2^-$  and  $\text{Ph}_3\text{P}^+-\text{CHPh}^-$  with adamantanone inside the NMR probe in different solvents (toluene, cumene, THF/toluene and  $\text{CH}_2\text{Cl}_2$ /toluene) at different temperatures (ranging from room temperature to 90 °C). All our attempts to observe  $^1\text{H}$  or  $^{31}\text{P}$  polarization were unsuccessful. The difficulty is that the recombination product (the zwitterion of type A) and the escape products (the alkoxide and the phosphonium ions) from the radical ion pair are not soluble in the solvents used and precipitate out in the NMR tube. Thus any polarization induced on protons or on phosphorus would have been left unnoticed. We also attempted CIDNP experiments using benzophenone and dibenzyl ketone as the carbonyl counterpart, but without success. In view of the above-mentioned difficulties, the absence to observe a CIDNP effect is therefore not unexpected.

Present work indicates that the initial one-electron transfer process<sup>11</sup> is involved as a competing pathway in the Wittig reaction of sterically hindered systems where reduction is predominantly observed over the usual olefin-forming Wittig reaction. The initial radical ion pair could, of course, also be involved in the Wittig pathway leading to olefins.<sup>12</sup>

#### Experimental Section

4-Hydroxyadamantan-2-one (2),<sup>8</sup> isopropyltriphenylphosphonium bromide,<sup>13</sup> and (diphenylmethyl)triphenylphosphonium bromide<sup>14</sup> were

(11) For one-electron transfer in Grignard reactions and metal hydride reactions, see: (a) Ashby, E. C.; Wiesmann, T. L. *J. Am. Chem. Soc.* **1978**, *100*, 189, 3101. (b) Ashby, E. C.; Goel, A. B.; DePriest, R. N. *Ibid.* **1980**, *102*, 7779. (c) Ashby, E. C.; Goel, A. B. *J. Org. Chem.* **1981**, *46*, 3934.

(12) We learned after completion of our work that Professor E. C. Ashby obtained in independent work direct ESR evidence for the one-electron-transfer mechanism. We are delighted to acknowledge his significant results.

(13) Fagerlund, U. H. M.; Idler, D. R. *J. Am. Chem. Soc.* **1957**, *79*, 6473.

prepared by known procedures. Adamantanone, methyltriphenylphosphonium bromide, benzophenone, and bicyclo[3.3.1]nonan-9-one are commercially available and were used as such. All solvents were of analytical grade and were used without any further purification. All  $^1\text{H}$  and  $^{13}\text{C}$  NMR spectra were recorded on a Varian XL-200 superconducting NMR spectrometer. All products were identified by comparison of the  $^{13}\text{C}$  and  $^1\text{H}$  NMR spectra with those of authentic samples.

**General Procedure.** To a stirred suspension of 20 mmol of alkyltriphenylphosphonium bromide in 50 mL of the specified solvent was added an equivalent amount of 2.2 M solution of *n*-butyllithium in hexane under  $\text{N}_2$  atmosphere. The mixture was stirred for 30 min<sup>15</sup> and 20 mmol of the ketone in 50 mL of the same solvent was added over a period of 30 min at room temperature. The reaction mixture was refluxed for 17 h and subsequently quenched with water. The precipitated phosphonium salt was filtered and washed with ether. The filtrate was subsequently washed with several portions of water and finally with saturated NaCl solution. Evaporation of the solvent after drying over anhydrous sodium sulfate gave the product(s). The product mixture was then analyzed by  $^1\text{H}$  and  $^{13}\text{C}$  NMR spectroscopy.

**CIDNP Experiments.**  $^1\text{H}$  NMR CIDNP experiments were conducted in the probe of a Varian Associates A56/60 spectrometer, and  $^{31}\text{P}$  NMR CIDNP experiments were performed in a Varian Associates XL-200 NMR spectrometer.

A pre-prepared solution (~10%) of the ylide in the appropriate solvent was placed in an NMR tube and equilibrated to a constant temperature inside the NMR probe. A concentrated solution of adamantanone (benzophenone or dibenzyl ketone) was introduced into the NMR tube through a syringe. The NMR signals were continuously monitored for 15 min.

**Acknowledgment.** Support of our work by the National Institutes of Health is gratefully acknowledged.

**Registry No.** 1, 700-58-3; 2, 81831-71-2; 3a, 875-72-9; 4, 51020-64-5; 5, 28644-55-5; 6a, 81831-71-2; 7, 17931-55-4; 8, 15598-80-8; 10, 119-61-9; 11, 91-01-0; 12, 781-33-9.

(14) Horner, v. L.; Lingnau, E. *Liebigs Ann. Chem.* **1955**, *591*, 135.

(15) When methylcyclopentane and methylcyclohexane were used as solvent, the BuLi and the phosphonium bromide were stirred at room temperature for 3 h.

## Sites of Photolytic Intermolecular Cross-Linking between Fatty Acyl Chains in Phospholipids Carrying a Photoactivable Carbene Precursor

Ramachandran Radhakrishnan, Catherine E. Costello, and H. Gobind Khorana\*

Contribution from the Departments of Chemistry and Biology, Massachusetts Institute of Technology, Cambridge, Massachusetts 02139. Received September 2, 1981

**Abstract:** A number of *sn*-glycero-3-phosphorylcholines containing the photosensitive  $\omega$ -[*m*-(3*H*-diazirino)phenoxy]undecanoyl group in the *sn*-2 position and a deuterated palmitic or stearic acid with both deuteriums on specific carbon atoms along the hydrocarbon chain in the *sn*-1 position were synthesized. Photolysis of either sonicated vesicles or multilamellar dispersions prepared from these synthetic phospholipids gave extensive intermolecularly cross-linked products. The distribution of the sites of cross-linking was determined by an analysis of cross-linked dimeric fatty esters by using low-resolution electron impact mass spectrometry. The predominance of the benzylic cleavage with a  $\gamma$ -hydrogen abstraction in the mass spectra of these diesters rendered such a quantitation relatively easy. Mass spectral analysis showed that there is a broad distribution in the cross-linking positions along the deuterated *sn*-1 chain, with the amount of cross-linking increasing toward the hydrophobic core of the bilayer. These results are in agreement with the conformational mobility of the fatty acyl chains and the localization of the photosensitive diazirinophenoxy group in the middle of the bilayer.

An understanding of phospholipid-phospholipid and phospholipid-protein interactions is of central importance in studies of biological membranes. An organochemical approach to such studies has been described which aims at the identification of the

interacting membrane components by formation of covalent cross-links between them. The approach involves the synthesis of phospholipids containing photoactivatable carbene or nitrene precursors as constituents of the fatty acyl chains.<sup>1,2</sup> Photolysis

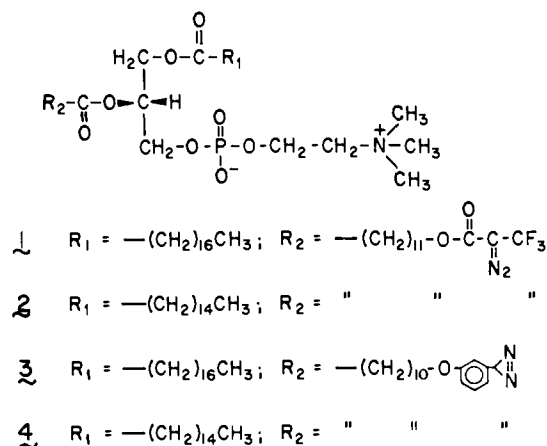
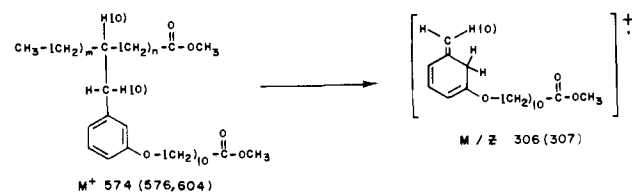


**Figure 1.** Synthetic mixed 1,2-diacylphosphatidylcholines carrying carbene precursors as photoactive groups. The phospholipids are prepared from 1-acyl-*sn*-glycero-3-phosphorylcholines by acylation with fatty acyl anhydrides containing photoactive groups in the hydrocarbon chains.

**Scheme I. Benzylic Cleavage in the Mass Spectra of the Cross-Linked Fatty Acid Esters**



of unilamellar vesicles prepared from phospholipids carrying the carbene precursors (Figure 1) was demonstrated to give intermolecularly cross-linked products as expected from the insertion of the reactive carbene intermediate into C-H bonds of the fatty acyl chains of neighboring phospholipid molecules.<sup>2</sup> In a further study with a set of phospholipids carrying a palmitoyl or stearoyl chain in the *sn*-1 position and  $\omega$ -( $\beta,\beta,\beta$ -trifluoro- $\alpha$ -diazopropionyloxy)-fatty acyl chain of varying lengths in the *sn*-2 position (**1**, **2**), a mass spectrometric analysis was carried out to determine the distribution of cross-links.<sup>3</sup> This study revealed that cross-linking occurred within the bilayer and that there was in fact a correspondence between the position of maximum cross-linking along the acceptor chain and the length of the fatty acid carrying the photolabel. A similar study with phospholipids carrying aryldiazirines **3** and **4** (Figure 1) would clearly be very informative. The nature of this carbene precursor is quite different from the trifluorodiazopropionate in characteristics such as size, structure, and stability. A correlation between the location of the photolabel and the cross-linking positions should provide a guide in studies of the topography of membrane proteins that are embedded in the phospholipid bilayer.

We have therefore prepared a set of phospholipids carrying aryldiazirines and, following their photolyses, have analyzed the sites of cross-linking by mass spectrometry. Specifically deuterated palmitic or stearic acid residues were incorporated into the *sn*-1 position of the phospholipids used in this study to take advantage of the prominence of the ion arising by benzylic cleavage of the C-C bond formed in the insertion process (Scheme I), a fragment retaining the hydrogen from the C-H bond into which the insertion occurred.

Since the acceptor chain carried deuterium at specific positions, the amount of insertion at this carbon could be calculated because the benzylic fragment occurs one mass unit higher in the mass

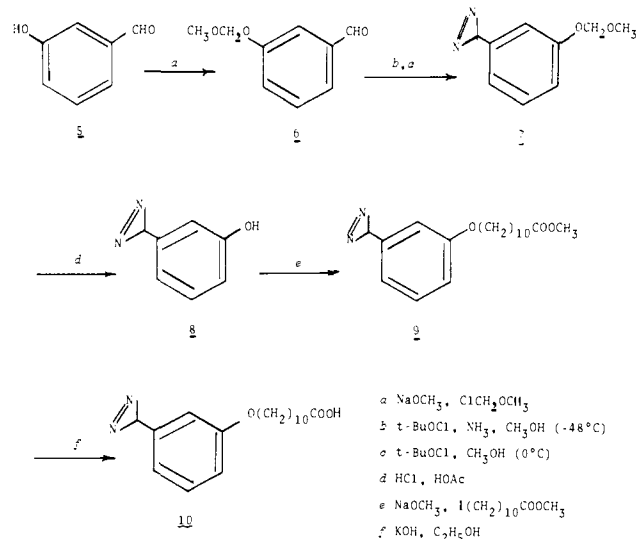


**Figure 2.** Synthetic pathway for  $\omega$ -[*m*-(3*H*-diazirino)phenoxy]undecanoic acid (**10**).

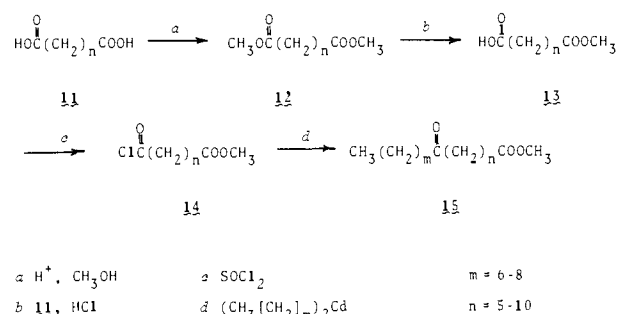


**Figure 3.** Synthetic pathway for keto fatty acid methyl esters **15**.

spectra of products formed by insertion into the C-D bond. The benzylic fragment is the result of a rearrangement process involving transfer of a hydrogen from the alkyl chain, and our model studies have shown that the hydrogen transfer has sufficient specificity to permit the assessment of the distribution of insertion points, even though the observed labeling pattern is broadened over what would have been the case for simple cleavage. The assessment of cross-linking sites obtained by this method shows that there is a distribution in the positions of cross-linking that is similar to but wider than that observed earlier.<sup>3</sup> The results obtained clearly indicate that the photolabel is positioned in the middle of the bilayer. Brief reports of this work have appeared previously.<sup>4,5</sup>

**Synthesis of  $\omega$ -[*m*-(3*H*-Diazirino)phenoxy]undecanoic Acid (**10**).** The requirements for the preparations of the phospholipids by the general method described previously are (1) fatty acids carrying the diazirinophenoxy groups in the  $\omega$ -position and (2) palmitic or stearic acids containing two deuteriums at specific positions along the hydrocarbon chain.

The synthesis of  $\omega$ -[*m*-(3*H*-diazirino)phenoxy]undecanoic acid (**10**) was carried out as shown in Figure 2.

The protected phenolic aldehyde **6** was prepared from *m*-hydroxybenzaldehyde (**5**) by alkylation with chlorodimethyl ether. This was converted to the 3*H*-diazirine **7** by the method of Schmitz.<sup>6</sup> Deblocking was achieved by treatment with stoichiometric amounts of 1 N HCl in glacial acetic acid. The phenolic diazirine **8** thus obtained was converted to the fatty acid **10** by an alkylation and ester hydrolysis.

**Synthesis of Specifically Dideuterated Palmitic or Stearic Acids.** Keto fatty acids with the oxo group in varying positions along the

(1) Gupta, C. M.; Radhakrishnan, R.; Khorana, H. G. *Proc. Natl. Acad. Sci. U.S.A.* **1977**, *74*, 315.

(2) Gupta, C. M.; Radhakrishnan, R.; Gerber, G. E.; Olson, W. L.; Quay, S. C.; Khorana, H. G. *Proc. Natl. Acad. Sci. U.S.A.* **1979**, *76*, 2595.

(3) Gupta, C. M.; Costello, C. E.; Khorana, H. G. *Proc. Natl. Acad. Sci. U.S.A.* **1979**, *76*, 3139.

(4) Radhakrishnan, R.; Gupta, C. M.; Erni, B.; Curatolo, W.; Robson, R. J.; Majumdar, A.; Ross, A. H.; Takagaki, Y.; Khorana, H. G. *Ann. N.Y. Acad. Sci.* **1980**, *346*, 165.

(5) Radhakrishnan, R.; Costello, C. E.; Khorana, H. G. XIth International Congress of Biochemistry, Toronto, Canada, 1979; Abstr. 05-R-54.

(6) Schmitz, E. *Chem. Ber.* **1962**, *95*, 688.

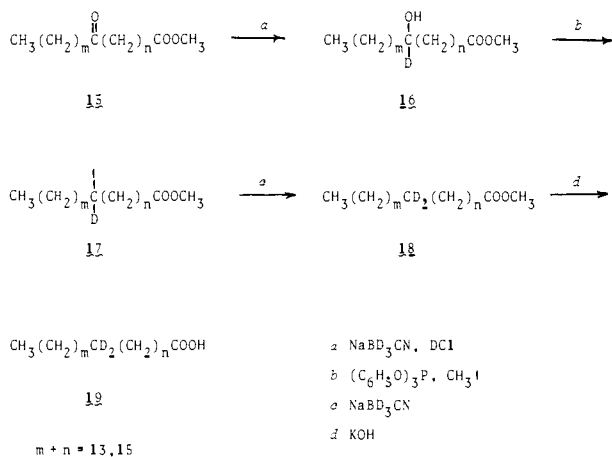


Figure 4. Pathway for reduction of keto fatty acid methyl esters.

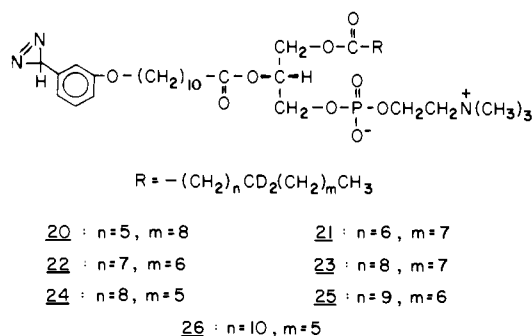


Figure 5. Structures of the synthetic deuterated photolabeled phospholipids used in this study.

chain served as the precursors for the dideuterated acids. These oxo acids were prepared from the  $\omega$ -dicarboxylic acids following the procedure of Hubbell et al.<sup>7</sup> (see Figure 3). Half-esters of 1, $\omega$ -dicarboxylic acids were prepared from the commercially available diacids **11** and their diesters **12** by an acid-catalyzed equilibration. These half-esters **13** were converted to their acid chlorides **14** and were condensed with alkylcadmium reagent to give the oxo fatty esters **15**. The specifically dideuterated palmitic or stearic acids were prepared by the deoxygenation of the ketone moiety of the oxo acids,<sup>8,9</sup> as shown in Figure 4. The keto esters **15** were reduced with sodium cyanoborodeuteride under acidic conditions. The resulting deuterated alcohols **16** were converted to the iodides by treatment with triphenoxyphosphonium methiodide. The secondary iodides **17** were once more reduced with sodium cyanoborodeuteride, and the fatty esters **18** were subsequently hydrolyzed to the dideuterated fatty acids.

**Phospholipids.** The mixed acyl lecithins containing the deuterated acids in the *sn*-1 chain and the photolabeled fatty acid in the *sn*-2 chain were synthesized as described previously.<sup>10</sup> The set of synthetic phospholipids prepared **20–26** appear in Figure 5.

## Experimental Section

**Materials.** 11-Bromoundecanoic acid, 4-dimethylaminopyridine, and all the 1, $\omega$ -dicarboxylic acids used in this study were purchased from Aldrich Chemical Co. Sodium cyanotri-deuteride borate was purchased from Aldrich or Ventron. Sodium methoxide was obtained from Fisher Scientific Co. Magnesium turnings were from Eastman. 10-Bromodecanoic acid was obtained from K & K. *tert*-Butyl hypochlorite was purchased from Frenon Chemicals. Chlorodimethyl ether was from Pfaltz and Bauer Co. Alkylphenols were obtained from Aldrich. Sources

for other materials have been described previously.<sup>2</sup>

**General Methods.** Melting points are uncorrected. Infrared spectra were recorded on a Beckman Model 4210 spectrophotometer. <sup>1</sup>H NMR spectra were recorded with a Varian T-60 spectrometer on samples in CDCl<sub>3</sub>. Chemical shifts are recorded in  $\delta$  with Me<sub>4</sub>Si as an internal standard. UV spectra were recorded in cyclohexane with a Cary Model 15 spectrophotometer. Purity of the intermediates, fatty acids, and phospholipids was routinely checked by thin-layer chromatography (TLC) with Merck silica gel plates. Unless indicated otherwise, petroleum ether (bp 35–60 °C)/ethyl ether (4:1, v/v) was used as the solvent system with fatty acids and diazirine intermediates. With phospholipids, chloroform/methanol/water (65:25:4, v/v/v) was used as the solvent system. Preparative TLC was performed with Merck plates (500  $\mu$ m thick) and appropriate solvents. The phospholipids were visualized by the molybdenum blue spray.<sup>11</sup> For the purification of phospholipids by column chromatography, 20–25 g of silica gel G (30–70 mesh) was used per mmol of phospholipid synthesized. Fatty acids were removed by washing the column with chloroform (about 500 mL/mmol scale reaction), and the phospholipid was then eluted with CHCl<sub>3</sub>/CH<sub>3</sub>OH (1:1, v/v). Sephadex LH-20 (25–100- $\mu$ m beads) chromatography on a 2.5  $\times$  100 cm column with CHCl<sub>3</sub>/CH<sub>3</sub>OH (1:1, v/v) as the eluant was used for the purification of phospholipids, separation of photolysis products, and the isolation of pure cross-linked dimeric fatty esters. Generally diacylphosphatidylcholines eluted faster than monoacylphosphatidylcholines and the fatty acids. The separation between lecithins and lysolecithins was marginal, but the fatty acids separated quite well from the phospholipids. The synthetic photolabeled deuterated phospholipids were purified by preparative TLC after Sephadex LH-20 column chromatography. Preparative HPLC of *m*-(methoxymethoxy)phenyl-3H-diazirine (**7**) was performed on a Waters Associates Prep 500 system with a Waters Prep PAK-500/silica cartridge (30  $\times$  5.7) as the column material and isooctane containing 1–2% diethyl ether (v/v) as the eluant at a flow rate of 250 mL/min. A refractive index detector was used to monitor the fractions. Analytical HPLC was performed on a Waters  $\mu$ Porasil column (39  $\times$  0.36) with isooctane containing 1–2% diethyl ether as the eluant at a flow rate of 4 mL/min.

**Mass Spectrometry.** Experimental conditions for gas chromatographic mass spectrometry (GC/MS), high-resolution electron-impact mass spectrometry (HRMS), and field desorption mass spectrometry (FDMS) were as described previously.<sup>3</sup> Deuterium incorporated in the benzylic fragment of the model compounds was determined in a GC/MS experiment by use of accelerating voltage scans with the Hitachi RMU-6L. Accuracy of this method is  $\pm 3\%$  of the observed value. The accurate peak intensity data on which the distribution of cross-linked products was calculated were obtained with the Varian MAT 731 instrument by slow scans over 2% of the accelerating voltage to cover the mass range  $m/z$  304–310. Values reported are the average of 10 or more scans. Standard deviation of these measurements was  $\pm 0.3\%$ . Data were obtained for samples admitted via the direct insertion probe heated to 80 °C for the diesters containing palmitate and 110 °C for those having stearate. Ion source temperature was 200 °C, accelerating voltage 8 kV, and electron energy 70 eV.

**Chemical Syntheses. Preparation of [*m*-(Methoxymethoxy)phenyl]-3H-diazirine (**7**).** To methanol (225 mL) cooled to –40 °C was added precondensed ammonia (75 mL) to make the solution approximately 10 N. A solution of *tert*-butyl hypochlorite (30 mL) in *tert*-butyl alcohol (30 mL) was added dropwise over a period of 1 h while the reaction mixture was stirred magnetically. To the resulting chloramine solution was added 40.0 g (0.25 mol) of the protected phenolic aldehyde **6**<sup>12</sup> and the mixture was allowed to warm up slowly. The total reaction time varied from 36 to 48 h. Ammonia and solvent were removed under an aspirator, and the residue was dried in vacuo. The semisolid residue thus obtained was suspended in reagent grade methanol (100 mL), cooled to 0 °C, and treated with a solution of *tert*-butyl hypochlorite (10 mL) in *tert*-butyl alcohol (25 mL) for 3 h. TLC indicated the formation of the diazirine as the fastest running component, and this was confirmed by the characteristic UV absorption of an aliquot of the reaction mixture. The mixture was poured into 15% (w/v) aqueous solution of sodium metabisulfite (600 mL), and the crude product was extracted with petroleum ether (3  $\times$  100 mL). The organic layer was dried (Na<sub>2</sub>SO<sub>4</sub>) and evaporated. The oily residue was chromatographed on a silicic acid column. Elution with petroleum ether containing 5% diethyl ether afforded 9.0 g of the aryldiazirine contaminated with a closely running

(7) Hubbell, W. L.; McConnell, H. M. *J. Am. Chem. Soc.* **1971**, *93*, 314.

(8) Borch, R. F.; Bernstein, M. D.; Durst, H. D. *J. Am. Chem. Soc.* **1971**, *93*, 2897.

(9) Hutchins, R. O.; Raryanoff, B. E.; Milewski, C. A. *J. Chem. Soc., Chem. Commun.* **1971**, 1097.

(10) Radhakrishnan, R.; Robson, R. J.; Takagaki, Y.; Khorana, H. G. *Methods Enzymol.* **1981**, *72D*, 408.

(11) Groswami, S. K.; Frey, C. F. *J. Lipid Res.* **1971**, *12*, 509.

(12) *m*-(Methoxymethoxy)benzaldehyde (**6**) was prepared by the condensation of the phenoxide generated from *m*-hydroxybenzaldehyde (**5**) with chlorodimethyl ether. The product was routinely purified by silicic acid column chromatography. Spectral characteristics were consistent with the structure for this compound.

component. Further purification was achieved by preparative HPLC to yield 4.1 g of pure diazirine as a colorless liquid: IR (Nujol) 1610, 1590  $\text{cm}^{-1}$ ; UV<sub>max</sub> (cyclohexane) 362 nm; ( $\epsilon$  285);  $^1\text{H NMR}$  ( $\text{CDCl}_3$ )  $\delta$  5.6–7.2 (m, 4 H), 2.3 (s, 1 H). Diazirine 7 is probably not thermally stable enough for GC/MS analysis and would be too volatile for introduction via direct insertion probe. However, the ethyl ester of  $\omega$ -[*m*-(3*H*-diazirino)phenoxy]undecanoic acid (**10**) was analyzed by low-resolution electron-impact mass spectrometry using an unheated direct insertion probe at an ion source temperature of 150 °C: obsd *m/z* (rel intensity) 88 (100), 101 (36), 107 (63), 108 (57), 133 (31), 147 (21), 289 (17), 346 (14,  $\text{M}^+$ ).

**Preparation of Keto Fatty Acid Esters.** Commercially available 1, $\omega$ -dicarboxylic acids served as starting material. The methodology employed is illustrated with reference to the preparation of methyl 9-ketopalmitate (**15**, *m* = 6, *n* = 7).

**Preparation of Azelaic Half Methyl Ester (13, *n* = 7).** To a mixture of azelaic acid dimethyl ester (**13**, *n* = 7) (16.4 g, 0.076 mol) and azelaic acid (**13**, *n* = 7) (12.4 g, 0.066 mol) in di-*n*-butyl ether (40 mL) was added concentrated HCl (3.32 mL), and the mixture was heated to reflux with stirring. After 30 min, methanol (6 mL) was added and the heating continued for an additional 2 h. TLC (ether) showed the monoester as the major component of the reaction mixture. The mixture was cooled, and the solvents were removed with an aspirator. The residual viscous mass was stirred with petroleum ether (200 mL) and allowed to stand for 2 h. The precipitated dicarboxylic acid was removed by filtration. The filtrate was transferred to a separatory funnel, and the half-ester was extracted with 0.4 M aqueous sodium carbonate (3  $\times$  100 mL). The aqueous extract was neutralized with HCl and partitioned with ether. Evaporation of the organic layer gave 12.2 g of the monoester **13** (*n* = 7) as a syrup; IR (Nujol) 1710, 1745  $\text{cm}^{-1}$ .

**Preparation of  $\omega$ -Carbomethoxyoctanoyl Chloride (14, *n* = 7).** The half-ester from above (12.2 g, 0.06 mol) was treated with thionyl chloride (14.2 g, 0.12 mol), and the mixture was stirred magnetically at ambient temperature. After overnight reaction, the excess reagent was removed under an aspirator and the residue was dried in vacuo to give 10.0 g of the acid chloride **14** as a liquid; IR (neat) 1750, 1800  $\text{cm}^{-1}$ .

**Preparation of Methyl 9-Ketopalmitate (15, *m* = 6, *n* = 7).** Magnesium turnings (1.43 g, 0.06 mol) were placed in a three-necked flask fitted with a reflux condenser, addition funnel, and nitrogen inlet. A stream of nitrogen was allowed to sweep through the system to remove any oxygen. Then anhydrous ether (100 mL) was added and the nitrogen flush continued for 0.5 h. A solution of 1-bromoheptane (10.56 g, 0.059 mol) in anhydrous ether (50 mL) was added, and the mixture was refluxed for 1 h, until almost the complete disappearance of magnesium. Powdered anhydrous cadmium chloride (5.4 g, 0.03 mol) was added, and the mixture was refluxed for an additional 45 min, when a bulky precipitate formed. The mixture was cooled to room temperature, and ether was distilled off under nitrogen. The residue was suspended in dry benzene (100 mL) and cooled in ice. To the benzene solution of the organocadmium derivative was added a solution of the acid chloride (**14**, *n* = 7) (13 g, 0.059 mol) in dry benzene (50 mL) over a 10-min period. The mixture was refluxed for 1.5 h. After the reaction period, the mixture was cooled in ice water (10 mL) and an excess of 0.1 N  $\text{H}_2\text{SO}_4$  was added until two layers formed. The benzene layer was washed once with water (100 mL). The organic layer was dried ( $\text{Na}_2\text{SO}_4$ ) and evaporated. The residue was crystallized from petroleum ether to give 12.8 g of colorless crystals: mp 37–38 °C (lit.<sup>13</sup> mp 37.6–38.8 °C); IR (KBr) 1710  $\text{cm}^{-1}$ .

**General Method of Preparation of Specifically Dideuterated Fatty Esters. (a) Reduction of Keto Fatty Esters.** A trace of methyl orange (~5 mg) was dissolved in deuterium oxide (0.23 mL) and freshly distilled tetrahydrofuran (4.6 mL). To this solution was added in succession keto ester **15** (7 mmol) and sodium cyanoborodeuteride (7 mmol). This was followed by dropwise addition of  $\text{CH}_3\text{COOD}/\text{DCl}$  [prepared by mixing  $\text{D}_2\text{O}$  (0.7 mL) and distilled acetyl chloride (0.7 mL)] until a red color persisted. Increments of tetrahydrofuran (4.6 mL) were added, and the mixture was stirred magnetically at ambient temperature for 3 h. The reaction mixture was poured into a saturated aqueous solution of sodium chloride (100 mL), and the products were extracted with petroleum ether (2  $\times$  100 mL). The organic layers were combined, dried ( $\text{Na}_2\text{SO}_4$ ), and evaporated. The residue was crystallized from petroleum ether. Yields of the deuterated hydroxy esters **16** ranged from 70 to 80%. These were analyzed by GC/MS for deuterium content and found to be  $\geq 96\%$   $d_1$ .

**(b) Preparation of Iodo Fatty Esters (17).** A solution of the hydroxy esters **16** (4.9 mmol) in dry hexamethylphosphoramide (10 mL) was treated with triphenoxyphosphonium bromide (9.8 mmol), and the mixture was stirred at ambient temperature for 16 h. Excess reagent was decomposed by the addition of methanol (10 mL), and the mixture was

poured into a 5% aqueous sodium hydroxide solution (200 mL). The crude product was extracted with diethyl ether (2  $\times$  75 mL). The combined organic layer was dried ( $\text{Na}_2\text{SO}_4$ ) and evaporated. The residue was purified by silicic acid column chromatography. The iodo esters were obtained as colorless liquids in ~80% yield.

**(c) Preparation of Specifically Dideuterated Fatty Acid Esters (18).** A solution of the iodo ester **17** (0.004 mol) in dry hexamethylphosphoramide (10 mL) was treated with sodium cyanotrideuterio-borate (16 mmol), and the mixture was heated to 80 °C for 5 h. The reaction mixture was then cooled to room temperature and poured into an aqueous saturated sodium chloride solution (100 mL), and the crude product was extracted with ether (2  $\times$  75 mL). The combined organic layer was dried ( $\text{Na}_2\text{SO}_4$ ) and evaporated, and the residue was purified by silicic acid column chromatography. Yields of the dideuterated fatty acid esters **18** ranged from 80 to 90%. HRMS measurements on these compounds confirmed the elemental composition and position of deuterium substitution. The percent deuterium incorporation was based on the relative peak intensities observed for the  $\text{M}^+$ , ( $\text{M} + 1$ )<sup>+</sup>, and ( $\text{M} + 2$ )<sup>+</sup> ions in the GC/MS spectra. In each case, the deuterium content of the esters was shown to be  $\geq 92\%$   $d_2$ , the remainder being  $d_1$ .

**Phospholipid Vesicles or Dispersions and Their Photolyses. Vesicles.** A chloroform solution of the phospholipid was dried under nitrogen, and to the dry residue was added 0.01 M Tris-HCl, pH 7.6, containing 0.15 M KCl to a concentration of 3 mg/mL. After being flushed with nitrogen, the tube was sealed, vortexed for 2 min, and then sonicated in a bath-type sonicator (80 W, 80 KHz at 3.5 A) until a clear solution resulted (30–45 min). Sonications were generally conducted at room temperature.

**Multilamellar Dispersions.** Phospholipids in chloroform were dried under nitrogen, and any residual solvent was removed by continued evaporation in vacuo. To the dry residue was added 0.01 M Tris-HCl (pH 7.6) containing 0.15 M KCl (final concentration 3 mg/mL). The suspension was vortexed for 10–15 min. The liposomes thus obtained were used as such for photolysis.

**Photolysis and Separation of Products.** The vesicles or liposomes were transferred to a quartz vessel with a jacket through which circulated aqueous (2% w/v) potassium hydrogen phthalate solution. This chemical filter served to eliminate light <310 nm. The vessel was placed in the center of a Rayonet photochemical reactor equipped with 16 symmetrically placed RPR 3500-Å lamps. The temperature of the circulating filter was controlled by a thermostat. Progress of photolysis was followed by monitoring the disappearance of the characteristic UV absorption of the diazirine after extraction of the reaction mixture aliquots. Approximately 20–30 min of irradiation was required for the complete decomposition of the diazirine. After the completion of the photolysis, the reaction mixtures were extracted,<sup>14</sup> the organic phase was evaporated, and the residue, as a concentrated solution in  $\text{CHCl}_3/\text{CH}_3\text{OH}$  (1:1, v/v), was applied to a Sephadex LH-20 column (2.5  $\times$  100 cm). Elution was performed with the same solvent at a rate of about 60 mL/h. Fractions were monitored by their phosphorus content.<sup>15</sup>

**Transesterification of Phospholipids.** To a methanolic solution of the photolysis product (~2 mg/mL) was added 0.01 mL of 0.5 M sodium methoxide in methanol, and the mixture was stirred at room temperature for 4 h. After evaporation of the mixture, the residue was dissolved in chloroform (0.5 mL) and washed with 30 mM HCl (0.5 mL). The aqueous layer was removed, and the organic phase containing the methyl esters was washed twice with water (2  $\times$  0.5 mL). Removal of the solvent from the organic phase yielded the fatty esters, which were separated by use of the Sephadex column as described above (for structures of the cross-linked fatty esters, see Figure 7).

## Results

**Isolation and Characterization of Cross-Linked Fatty Esters.** It has been shown previously<sup>2</sup> that these photoactivatable phospholipids form sealed vesicles trapping solutes like [<sup>14</sup>C] glucose. The phase-transition temperatures of the synthetic analogues were consistently lower than the strictly straight-chain saturated phospholipids. Either small, sonicated vesicles or multilamellar dispersions of synthetic photolabeled phospholipids were photolyzed. The photolyses were conducted at, above, and below the phase-transition temperature of this lipid<sup>16</sup> (9 °C, determined for the undeuterated compound). Products were separated on a Sephadex LH-20 column. Analysis of material from sonicated vesicles on irradiation at 350 nm and separation of cross-linked

(14) Bligh, E. G.; Dyer, W. J. *Can. J. Biochem. Physiol.* **1959**, *37*, 911.

(15) Ames, B. N.; Dubin, D. T. *J. Biol. Chem.* **1960**, *235*, 769.

(16) Curatolo, W.; Radhakrishnan, R.; Gupta, C. M.; Khorana, H. G. *Biochemistry* **1981**, *20*, 1374.

(13) Oezeris, S. *Fette, Seifen, Anstrichm.* **1961**, *63*, 805.

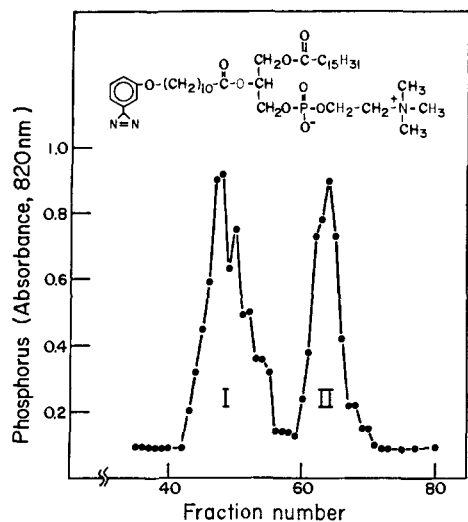


**Figure 6.** Sephadex LH-20 column elution profile (2.5 × 100 cm) of the products obtained from the photolysis of 1-palmitoyl-2-[ $\omega$ -(diazirinophenoxy)undecanoyl]phosphatidylcholine. Peak I accounted for 55% of the total phosphate-containing material and peak II, the remainder.

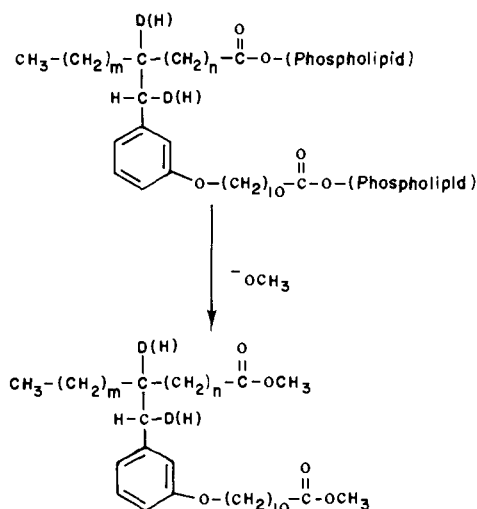


**Figure 7.** General structures of the cross-linked products obtained on photolysis of phospholipids containing  $\omega$ -(*m*-diazirinophenoxy) groups in the *sn*-2 fatty acyl chain and the products obtained after transesterification. The isomer drawn illustrates insertion at the labeled carbon atom of the deuterium-labeled compound. Other isomers are, of course, also present in the mixture obtained in the photolysis experiments.

products by the sizing column showed that an approximate 50–55% of the starting material appeared in the presumed cross-linked products of high molecular weight (peak I of Figure 6), the remainder being in peak II, the monomeric fraction. In the case of multilamellar structures, radioactivity and phosphate determination showed an approximate 65% cross-linking. Both the fractions were analyzed by transesterification and mass spectrometry of fatty esters obtained.<sup>2</sup> The monomeric fraction when analyzed after transesterification showed approximately 5% of the material in peak II arose from *sn*-1 to *sn*-2 chain cross-linking. The rest of the material arose from the reaction of the carbene intermediate with water/oxygen or the decomposition of the isomerized diazo compound. Material in peak I gave mixtures of monomeric and dimeric fatty esters, which were separated on a Sephadex LH-20 column. The cross-linked dimeric esters in each case had molecular weights consistent with the general structure assigned as shown in Figure 7.

**Mass Spectrometry of Fatty Acid Esters.** Field desorption mass spectra of the products had molecular ions appropriate for the cross-linked fatty esters. Minor components were the products arising from carbene–carbene dimerization. Trace amounts of higher molecular weight materials were present. No significant

**Table I.** High-Resolution Electron Impact Data for Selected Ions in the Mass Spectra of Diesters Obtained after Irradiation and Transesterification of Synthetic Phospholipids

compd	<i>m/z</i>		phospholipid <sup>a</sup>
	calcd	obsd	
C <sub>36</sub> H <sub>62</sub> O <sub>5</sub>	574.4597	574.4622	3
C <sub>36</sub> H <sub>60</sub> O <sub>5</sub> D <sub>2</sub>	576.4723	576.4703	20
C <sub>38</sub> H <sub>64</sub> O <sub>5</sub> D <sub>2</sub>	604.5036	604.5049	25
C <sub>38</sub> H <sub>56</sub> O <sub>6</sub>	608.4076	608.4065	dimer from 25
C <sub>19</sub> H <sub>30</sub> O <sub>3</sub>	306.2195	306.2207	3
		306.2224	20
		306.2180	25
C <sub>18</sub> <sup>13</sup> CH <sub>30</sub> O <sub>3</sub>	307.2229	307.2239	3
C <sub>19</sub> H <sub>29</sub> O <sub>3</sub> D	307.2258	307.2248	20
		307.2250	25

<sup>a</sup> See discussion.

**Table II.** Ion Abundances in Diester Mass Spectra Used for Assessment of Intermolecular Insertion Point Distributions

phospholipid <sup>a</sup> (label at C-)	obsd ratio (307/306) × 100	excess <i>m/z</i> 307 (307/306) × 100	diester <i>M<sub>r</sub></i>
3	21.2 <sup>b</sup>		574
20 (C-7)	36.8	15.6	576
21 (C-8)	37.4	16.2	576
	37.5	16.3	576
	38.5	17.3	576
22 (C-9)	38.2	17.0	576
23 (C-10)	39.7	18.5	604
24 (C-10)	41.3	20.2	576
25 (C-11)	44.4	23.2	604
26 (C-12)	45.7	24.5	604

<sup>a</sup> See discussion. <sup>b</sup> Theoretical abundance of (*M* + 1) for C<sub>19</sub>H<sub>30</sub>O<sub>3</sub> (*m/z* 306) = 21.2%, as observed.

fragment ions appeared in the FD spectra of these compounds. The cross-linked esters had molecular ions at *m/z* 574, 576, and 604 for the unlabeled palmitoyl, the *d*<sub>2</sub>-labeled palmitoyl and the *d*<sub>2</sub>-labeled stearoyl insertion products, respectively, and *m/z* 608 for the carbene–carbene dimer.

Complete high-resolution electron-impact mass spectra were obtained for the transesterified irradiation products after their purity had been determined from the FD spectra. Results obtained for products from unlabeled palmitoyl-, 8,8-dideuteriopalmityl-, and (10,10-dideuteriostearoyl)(diazirinophenoxyundecanoyl)-phosphatidylcholine were typical; data for their molecular ions and benzylic cleavage ions appear in Table I. The exact mass measurements of the molecular ions provided elemental compositions that indicated that cross-linking had occurred. Ions derived from the acceptor chain had low abundance in the electron impact mass spectrum, and their further cleavage made it difficult to use their abundances to determine the sites of cross-linking. Cleavage at the benzylic site accompanied by hydrogen transfer, however, resulted in an ion at *m/z* 306 in the spectrum of the unlabeled diester, whose abundance made it quite suitable for isotope measurements. The elemental composition determined at high resolution (Table I) is consistent with this assignment as a benzylic rearrangement ion. A study of the relative intensities of the *m/z* 306 and 307 peaks would therefore reflect the extent of deuterium transfer to the benzylic position during carbene insertion into an acceptor chain carrying a label. For determination of the distribution of cross-linking sites, carbon atoms 7–12 were selectively deuterated in the acceptor chain. After photolysis and transesterification, the cross-linked esters were analyzed by low-resolution electron-impact mass spectral scans. The spectra of the products obtained from unlabeled palmitoyl- and (9,9-dideuteriopalmityl)(diazirinophenoxyundecanoyl)phosphatidylcholine are shown in Figure 8.

The abundances of *m/z* 306 and 307 were accurately determined by accelerating voltage scans over the mass range *m/z* 304–310. Results reported are the average of 10 or more con-

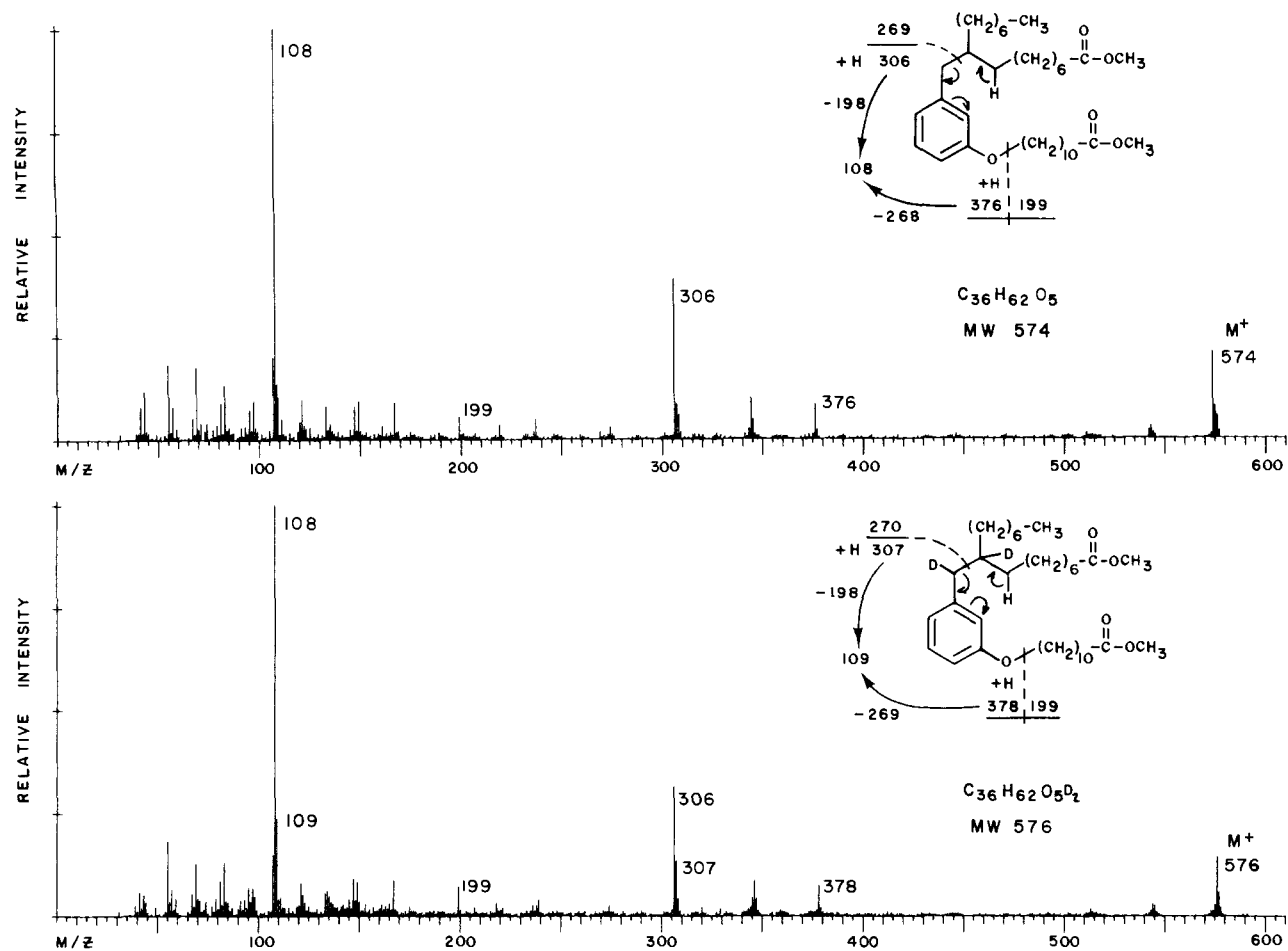


**Figure 8.** Low-resolution electron impact mass spectra of the diesters obtained by the photolysis of phospholipids **3** and **22** followed by transesterification of intermolecularly cross-linked products. Each sample is a mixture of isomers that differ in the position of the cross-link (for structure of phospholipids, see Figures 1 and 5).

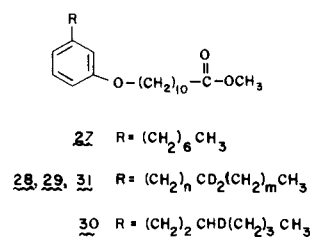


**Figure 9.** Structures of the  $\omega$ -[(*m*-heptyl)phenoxy]undecanoic acid methyl esters prepared as model compounds.

secutive scans with a standard deviation of  $\pm 0.3\%$ . The data are summarized in Table II.

#### Model Compounds Confirm $\gamma$ -Hydrogen Abstraction Pathway.

In order to demonstrate the specificity of the abstraction for the compounds in this study, we initiated a companion study in which a series of labeled alkyl phenols (**21**) were prepared and reacted with  $\omega$ -iodoundecanoic acid methyl ester to provide the compounds **27–31** (Figure 9). The low-resolution electron-impact spectra of the unlabeled compound **27** and the  $\gamma,\gamma$ -labeled compound **29** shown in Figure 10 are typical. A comparison of the two spectra confirms that the benzylic cleavage and  $\gamma$ -hydrogen abstraction upon ionization of the nondeuterated compound results in an ion of  $m/z$  306 and of the deuterated compound in an ion of  $m/z$  307. Further cleavage of the  $m/z$  306 or 307 ions with a loss of  $(\text{CH}_2)_{10}\text{COOCH}_3$  leads to ions of  $m/z$  108 and 109, respectively. Because ions in the cluster at  $m/z$  107–110 can arise via two or more fragmentation pathways, the labeling pattern is not so clear as it is at  $m/z$  306–308. These compounds were not isolated, so the ratios of their isotopic abundances at  $m/z$  306/307 were obtained by accelerating voltage scans over the mass range  $m/z$  300–310 during elution of the gas chromatographic peak. The

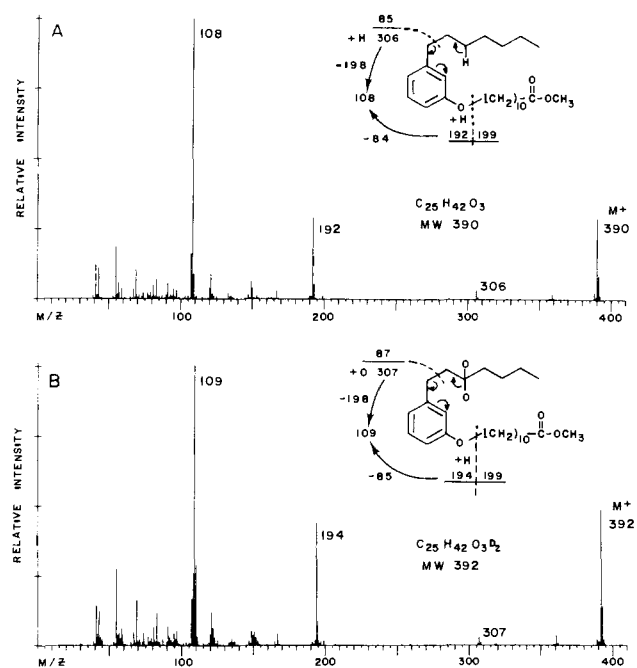
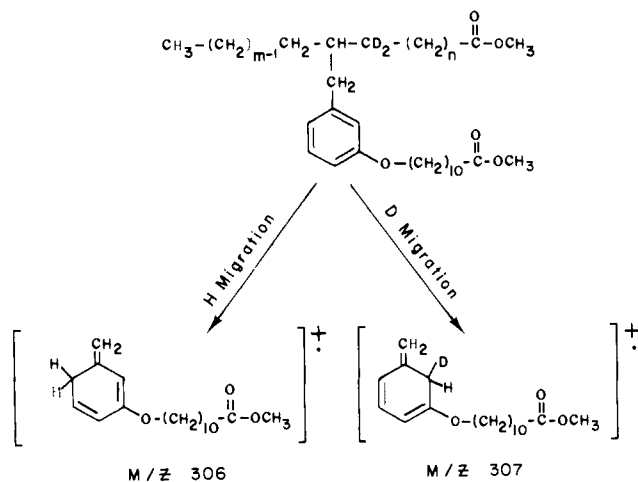


**Figure 10.** Low-resolution electron impact mass spectra obtained in GC/MS analysis of the model compounds **27**, which was unlabeled, and **29**, the  $\gamma,\gamma$ -labeled ether.

faster scan speeds and lower capability of the mass spectrometer employed for these measurements resulted in less accuracy than was obtained for the diester relative abundance measurements in Table I.

Scheme II. Possible Rearrangements of Diester Isomer in which Insertion Has Occurred Adjacent to the Labeled Carbon



### Discussion

The diazirines are unique candidates for photoaffinity labeling due to their remarkable stability,<sup>17,18</sup> their longer wavelength absorption, and their relative ease of photolysis. Bayley and Knowles<sup>19</sup> have shown that aryldiazirines added to a phospholipid bilayer underwent cross-linking to phospholipids on photolysis. We have shown here that aryldiazirines present as an integral part of fatty acyl chains underwent covalent attachment to the neighboring chain in model membrane systems on irradiation. Brunner and Richards have demonstrated similar cross-linking reactions in bilayers composed of phospholipids carrying aryl-(trifluoromethyl)diazirines as photolabels and acceptor lipids.<sup>20,21</sup> (The structures of the expected cross-linked products for the phospholipids used in this study are shown in Figure 7.) In our experiments, the product contained 5% of the material resulting from *sn*-1 to *sn*-2 insertion in the same molecule. The oligomeric material in peak I (Figure 6) contained primarily compounds (~75–80% of the cross-linked product) arising from the insertion of the carbene into the fatty acyl chain of a second molecule. Some dimeric phospholipid arising via a carbene–carbene dimerization could also be detected, but amounted to less than 10% of the cross-linked product. Very small amounts (5–10% of the cross-linked product) of still higher molecular weight materials were presumably present in this peak. Transesterification and gel exclusion provided reasonably pure dimeric fatty esters. Thus, the products of cross-linking arising via C–H insertion would be about 35–40%. Brunner and Richards<sup>20</sup> have reported that their carbene reagent reacted with saturated lipids to give up to a 20% yield. In the work with phenyldiazirine<sup>19</sup> added to liposomes in low concentrations, cross-linking yields of ~10% has been reported. In the present work cross-linking occurs in photoactivatable phospholipid vesicles where acceptor and donor molecules are the same, and therefore the apparently high yield of cross-linking is not inconsistent with the above studies. Table I contains HRMS data for peak I (Figure 6) from a typical experiment. The structures of the selected ions in the spectra of the cross-linked material prepared from phospholipids containing no deuterium in the *sn*-1 chain and that of the deuterated isomer in which insertion has occurred at the deuterated carbon atom are shown in Scheme I.

**Benzylic Cleavage of Diesters and  $\gamma$ -Hydrogen Abstraction.** Simple benzylic cleavage in the mass spectra of these compounds would result in an ion at *m/z* 305, which would shift to *m/z* 306

Table III. Ion Abundances in Mass Spectra of Model Compounds 27–31

ether (label)	obsd ratio (307/306) × 100	excess <i>m/z</i> 307 (307/306) × 100	% <i>d</i> <sub>1</sub> label
27	21 <sup>a</sup>	0	0
28 ( $\beta,\beta$ )	22	0	0
29 ( $\gamma,\gamma$ )	869	848	89
30 ( $\gamma$ )	131	110	52
31 ( $\delta,\delta$ )	38	17	14

<sup>a</sup> Theoretical abundance of (*M* + 1) for C<sub>19</sub>H<sub>30</sub>O<sub>3</sub> + 21.2%. Accuracy of GC/MS determination ±3%.

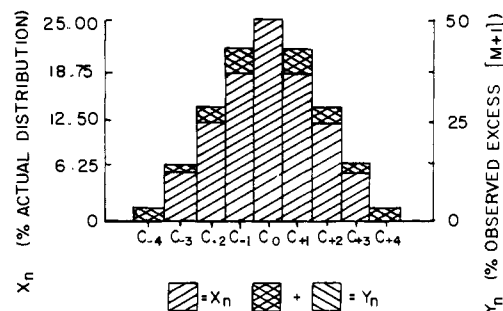


**Figure 11.** Theoretical distribution of normalized peak intensities of the (*M* + 1) ion, after removal of the <sup>13</sup>C contribution, for a fragment ion arising by cleavage accompanied by  $\gamma$ -H(D) transfer. For the purpose of constructing this figure, a distribution (1:2:3:4:3:2:1) was assumed for the insertion at the deuterium-labeled carbon and a 1:1 probability of deuterium transfer in the case where insertion occurred adjacent to the labeled site (see text).

if cross-linking occurred at the carbon bearing deuterium. However, previous work had indicated that in the spectra of aromatic ethers and phenols, particularly those of meta-substituted compounds, benzylic cleavage is accompanied by rearrangement of a hydrogen atom.<sup>22</sup> Rearrangement was the exclusive pathway observed for benzylic cleavage in the spectra of these compounds (Figure 8, Table I). In the case of alkyl-substituted phenols, it had been demonstrated that the hydrogen abstraction takes place primarily from the  $\gamma$  position.<sup>23</sup> The results of our experiments are meaningful only if similar specificity can be expected for these meta-substituted long-chain alkyl ethers. The two possible rearrangement ions that would have a 1:1 likelihood of occurrence in the spectra of the isomer resulting from the insertion at a carbon adjacent to labeled carbon are shown in Scheme II. A deuterium isotope effect on the rearrangement would result in a predominance of the *m/z* 306 resulting from H migration.

In order to evaluate the likelihood of rearrangement and its specificity, we carried out a study involving model compounds 27–31. These experiments demonstrated (Table III) that about 90% of the itinerant hydrogen migrates from the  $\gamma$  position and that there is no significant isotope effect.

**Determination of the Sites of Cross-Linking.** This specificity of benzylic cleavage and  $\gamma$ -hydrogen abstraction permits the assessment of the cross-link site distribution on the basis of the ratio of the abundances of *m/z* 306 and 307 in the spectra of the diesters. The possibility for transfer of a  $\gamma$ -deuterium atom broadens the observed distribution but does not change the position of the maximum. This fact becomes clear if one considers a theoretical distribution of insertion points such as is shown in Figure 11. In this figure, a possible distribution of insertion points about the preferred carbon, here designated C<sub>0</sub>, is indicated by the diagonally shaded bars to be 1:2:3:4:3:2:1. The incorporation of deuterium in the fragment ion being monitored can be due either to insertion at the carbon carrying the deuterium labels (C<sub>n</sub>), in which case the probability for transfer of deuterium to the portion of the molecule that gives rise to the fragment being monitored

(17) Smith, R. A. G.; Knowles, J. R. *J. Chem. Soc., Perkin Trans 2* **1975**, 686.

(18) Bradley, G. F.; Evans, B. L.; Stevens, I. D. R. *J. Chem. Soc., Perkin Trans 2*, **1977**, 1214.

(19) Bayley, H.; Knowles, J. R. *Biochemistry* **1978**, *17*, 2420.

(20) Brunner, J.; Richards, F. M. *J. Biol. Chem.* **1980**, *255*, 3319.

(21) Richards, F. M.; Brunner, J. *Ann. N.Y. Acad. Sci.* **1980**, *346*, 144.

(22) Oocolowitz, J. *Anal. Chem.* **1964**, *36*, 2177.

(23) Gorfinkel, M. I.; Ivanovskaia, L. Yu.; Koptys, Y. A. *Org. Mass. Spectrom.* **1969**, *2*, 273.

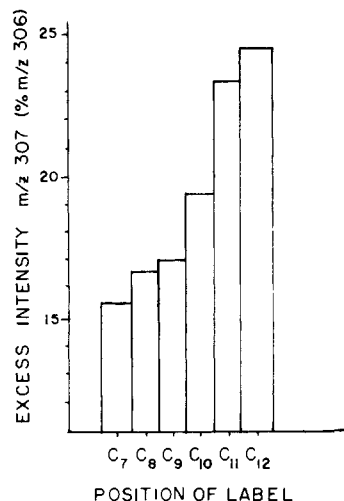


**Figure 12.** Distribution of normalized intensities of  $m/z$  307 in the mass spectra of the product diester mixtures resulting from photolysis and transesterification of phospholipids **3** and **20–26**. Correction for  $^{13}\text{C}$  has been made. The value shown for C-8 is the average of three C-8 labeling experiments and for C-10 the average of two, as shown in Table II.

is 100% for the insertion itself, or to insertion at the carbon adjacent to the labeled site ( $\text{C}_{n-1}$  or  $\text{C}_{n+1}$ ), in which case there is a 50% probability of labeling the fragment, depending on which of the neighboring carbon atoms is the source of the itinerant hydrogen. Therefore, in Figure 11 and in eq 1, if  $X_n = \%$  insertion at the labeled carbon  $\text{C}_n$ ,  $X_{n-1}$  and  $X_{n+1} = \%$  insertion at each of the adjacent carbon atoms, and  $Y_n = \%$  labeling observed for the fragment, then

$$Y_n = X_n + 0.5(X_{n-1} + X_{n+1}) \quad (1)$$

Since there is no hydrogen at the ester carbon ( $n = 1$ ), the total distribution of label will fall over the values  $n = 2$  to  $n = 16$  or  $n = 18$ , depending on the length of the fatty acyl chain. The total amount of labeling observed will then be the sum of the values of  $Y_n$ . It will be distributed symmetrically to one carbon on either side of the range where  $X_n$  had nonzero values. This is represented by the entire shaded area of Figure 11 (the diagonally hatched and cross-hatched areas together). The results obtained for **29** and **30** indicated that there is no significant isotope effect on the transfer. Since any isotope effect would lead to a lower rate of

deuterium transfer, this figure represents a "worst case" of broadening of the distribution due to  $\gamma$ -D migration. The fact that there is a contribution from a mass spectral rearrangement to the peak whose abundance is being used to monitor the insertion distribution therefore does not preclude use of this peak's abundance as a measure of the distribution of insertion points.

Figure 12 shows the distribution of intensities of  $m/z$  307 in the spectra of the diesters on the basis of the data in Table II. These results demonstrate that the probability for involvement of a specific carbon in cross-linking increases along the chain. Thus, we have shown that most of the cross-linking occurs in the middle of the bilayer.

It is clear from what is reported here and in the previous study<sup>2,3</sup> that the cross-linking in bilayers occurs by carbene insertion into a neighboring saturated fatty acyl chain. The photolabel did not cross-link in the polar head group, and the cross-linking was localized only in the hydrophobic region of the fatty acyl chain, with the extent of cross-linking increasing away from the polar carboxyl terminus. The broad distribution in cross-linking observed here is comparable to the recent findings on the order in artificial bilayers constructed from didodecyl phosphate with benzo-phenonecarboxylates as photochemical probes.<sup>24</sup> The correlation now shown should prove to be useful in the study of the topography of membrane-embedded proteins with phospholipids carrying less discriminant carbene precursors as an integral part of the membrane.

**Acknowledgment.** We are grateful to D. Kidwell for the synthesis of the labeled phenols from which the model compounds **27–31** were prepared and to Professor K. Biemann for many helpful discussions. This work is supported by Grant No. RR00317 from the NIH Division of Research Resources (awarded to K.B.) and Grant GM28289 and AI11479 of the National Institutes of Health, DHEW, and Grant PCM78-13713 of the National Science Foundation, Washington, D.C. (awarded to H.G.K.).

**Registry No.** **3**, 81814-99-5; **5**, 100-83-4; **6**, 13709-05-2; **7**, 80863-09-8; **10**, 80863-12-3; **13** ( $n = 7$ ), 2104-19-0; **14** ( $n = 7$ ), 56555-02-3; **15** ( $m = 6, n = 7$ ), 54527-11-6; **20**, 81830-38-8; **21**, 81815-00-1; **22**, 81815-01-2; **23**, 81815-02-3; **24**, 81815-03-4; **25**, 81815-04-5; **26**, 81815-05-6; **27**, 81815-06-7; **28**, 81815-07-8; **29**, 81815-08-9; **30**, 81815-09-0; **31**, 81815-10-3; 1-bromoheptane, 629-04-9.

(24) Czarniecki, M. F.; Breslow, R. *J. Am. Chem. Soc.* **1979**, *101*, 3675.